2009-09

Detailed design of a resonantly-enhanced axion-photon regeneration experiment

Mueller, Guido

Detailed design of a resonantly-enhanced axion-photon regeneration experiment

Guido Mueller,* Pierre Sikivie, and D.B. Tanner
Department of Physics, University of Florida, Gainesville, FL 32611, USA

Karl van Bibber†
Naval Postgraduate School, Monterey, CA 93943, USA

(Dated: February 20, 2013)

A resonantly-enhanced photon-regeneration experiment to search for the axion or axion-like particles is described. This experiment is a *shining light through walls* study, where photons travelling through a strong magnetic field are (in part) converted to axions; the axions can pass through an opaque wall and convert (in part) back to photons in a second region of strong magnetic field. The photon regeneration is enhanced by employing matched Fabry-Perot optical cavities, with one cavity within the axion generation magnet and the second within the photon regeneration magnet. Compared to simple single-pass photon regeneration, this technique would result in a gain of $(\mathcal{F}/\pi)^2$, where $\mathcal{F}$ is the finesse of each cavity. This gain could feasibly be as high as 10^{10}, corresponding to an improvement in the sensitivity to the axion-photon coupling, $g_{a\gamma\gamma}$, of order $(\mathcal{F}/\pi)^{1/2} \sim 300$. This improvement would enable, for the first time, a purely laboratory experiment to probe axion-photon couplings at a level competitive with, or superior to, limits from stellar evolution or solar axion searches. This report gives a detailed discussion of the scheme for actively controlling the two Fabry-Perot cavities and the laser frequencies, and describes the heterodyne signal detection system, with limits ultimately imposed by shot noise.

I. INTRODUCTION

The axion remains the most attractive solution to the strong-CP problem and is also one of two leading dark-matter candidates[1]. Recently, it has been realized that axions represent a fundamental underlying feature of string theories; there could be several or even a great number of axions or axion-like particles within any particular string theory[2].

Present constraints restrict the axion to have very small mass with mc^2 in the range between a μeV and a meV, making the axion extraordinarily weakly coupled to matter and radiation. Nevertheless, there is considerable ongoing experimental effort to search for axions. There are at least three distinct branches to the search. One may detect the axions which constitute the dark matter, observe axions emitted from the sun's burning core, or produce and observe axions employing purely laboratory methods. These last experiments do not depend on cosmological or astrophysical sources. All of the current efforts rely on the axion's coupling to two photons; indeed, all are based on the Primakoff effect by which one of the photons is virtual, whereby an axion can convert into a single real photon of the same energy (or *vice versa*) in a classical electromagnetic field, generally that of a large high-field superconducting magnet[3]. The coherent mixing of axions and photons over large spatial regions can compensate for the axion's extremely weak coupling to a degree sufficient to encourage the experimental campaigns, although it must be recognized that at the present time, there is no credible strategy to completely cover the remaining open parameter space for the axion mass, m_a, or its coupling to two photons, $g_{a\gamma\gamma}$.

The simplest and most unambiguous purely laboratory experiment to look for axions (or light scalars or pseudoscalars more generally) is photon regeneration (*shining light through the wall*)[4]. A laser beam traverses a magnetic field, and the field stimulates a small fraction of photons to convert to axions of the same energy. A material barrier easily blocks the primary laser beam; in contrast, the axion component of the beam travels through the wall unimpeded and enters a second identical arrangement of magnets. There the axions are converted with the same probability back to photons. Because the photon-regeneration rate goes as $g_{a\gamma\gamma}^4$, the sensitivity of the experiment is poor in its basic form, improved only by increasing the magnetic field strength or the length of the interaction regions. As initially suggested by Hoogeveen and Ziegenhagen[5] and briefly presented in a previous letter[6], very large gains may be realized in both the photon-regeneration rate, and the resulting limits on $g_{a\gamma\gamma}$ by introducing matched optical resonators in both the axion production and the photon regeneration magnetic field regions. In this longer report, we provide a detailed discussion of an experimental realization, particularly the scheme for locking two matched high-finesse optical resonators, the signal detection method, and the ultimate noise limits. Although challenging, the feasibility of the experiment relies on well-established technologies developed for example for laser interferometer gravitational-wave detectors[7].

Section II will summarize the relevant theory and phenomenology of the axion. Section III will discuss photon regeneration, and resonantly-enhanced photon regeneration, presenting experimental results for the former. Section

IV will describe the design and operation of the laser and optical cavity system, based on a 6+6 string of Fermilab dipole magnets. Section V will present projected results for this specific design.

II. THE AXION IN PARTICLE PHYSICS, ASTROPHYSICS AND COSMOLOGY

The QCD Lagrangian contains a term which violates both P and CP, the so-called *theta term*,

$$\mathcal{L}_\theta = \frac{\theta g_s^2}{32\pi^2} G^a_{\mu\nu} \tilde{G}^{a\mu\nu}, \tag{1}$$

where $G^a_{\mu\nu}$ is the gluonic field strength, $\tilde{G}^{a\mu\nu}$ is the dual of $G^a_{\mu\nu}$, g_s is the QCD gauge coupling, and θ is a phase angle unprescribed by the Standard Model. The fact that the strong interactions conserve P and CP to a very high degree, as evidenced by the upper bound on the neutron electric dipole moment, implies that $\bar{\theta} \equiv \theta - \arg\,(\det\, m_q) < 10^{-10}$. There is no reason within the Standard Model why $\bar{\theta}$ should be small. The absence of P and CP violations in the strong interaction constitutes therefore a puzzle, usually referred to as the strong CP problem. Peccei and Quinn[8] in 1977 discovered an elegant solution to this problem in which θ becomes a dynamical variable of the theory and is driven to its CP-conserving value by the non-perturbative effects which make QCD physics depend upon $\bar{\theta}$. The axion is the light pseudo-scalar particle which necessarily results from this theory[9]. It has a mass of

$$m_a = \frac{f_\pi m_\pi}{f_a} \cdot \frac{\sqrt{m_u m_d}}{m_u + m_d} \approx 0.6 \text{ eV} \left(\frac{10^7 \text{ GeV}}{f_a} \right) \tag{2}$$

and a coupling to two photons given by

$$\mathcal{L}_{a\gamma\gamma} = g_\gamma \cdot \frac{\alpha}{4\pi} \cdot \frac{a}{f_a} \cdot F_{\mu\nu} \tilde{F}^{\mu\nu} \ . \tag{3}$$

Here f_a is some large energy scale where PQ symmetry is spontaneously broken, and g_γ is a model-dependent parameter of the theory. In all grand-unified models, for example the Dine-Fischler-Srednicki-Zhitnitskii model (DFSZ)[10], $g_\gamma \approx 0.36$. In contrast, in the Kim-Shifman-Vainstein-Zhakarov (KSVZ) model[11], $g_\gamma \approx -0.97$. The axion-photon coupling is defined as $g_{a\gamma\gamma} \equiv \alpha |g_\gamma| / \pi f_a$; note that thus $g_{a\gamma\gamma} \propto m_a$ and limited explorations of axion models find that for a given mass, $g_{a\gamma\gamma}$ only varies over about an order of magnitude.

A sufficiently light axion would also be an excellent cold dark matter (CDM) candidate. The axion mass is bounded from below by a cosmological constraint, namely the requirement that the present axion cosmological energy density not exceed the critical density of the universe. From the vacuum-realignment axion production mechanism the present-day density is[12]

$$\rho_a^{vac}(t_0) \approx \rho_{crit}(t_0) \left(\frac{0.6 \cdot 10^{-5} \text{ eV}}{m_a} \right)^{7/6} \left(\frac{200 \text{ MeV}}{\Lambda_{QCD}} \right)^{3/4} \left(\frac{75 \text{ km/s} \cdot \text{Mpc}}{H_0} \right)^2 \tag{4}$$

where $\rho_{crit} \equiv 3H_0^2/8\pi G$ is the present critical energy density, H_0 is the present value of the Hubble constant and Λ_{QCD} is the QCD scale factor. Eq. (4) implies the bound $m_a > 0.6 \cdot 10^{-5}$ eV.

It should be noted that Eq. (4) only provides a rough estimate of the axion cosmological energy density. Uncertainties result from many sources; in particular, whether PQ symmetry-breaking occurred before or after inflation, the nature of the QCD phase transition, and the possibility of entropy production by late-decaying heavy particles. Assuming standard concordance cosmology, our estimate of the most likely value of the axion mass for which $\Omega_a = 0.22$ is $1.5 \cdot 10^{-5}$ eV, if inflation happens before the PQ phase transition. Nevertheless, given all uncertainties, the lower bound on the axion mass is nominally taken to be $m_a > 10^{-6}$ eV.

The mass of the axion is bounded from above by laboratory experiments and constraints from stellar evolution, the most severe being SN1987a[13], which limits the axion mass to $m_a < 1.6 \cdot 10^{-2}$ eV. The bound from SN1987a results from the duration of the neutrino pulse observed by the IMB and Kamioka detectors (about 20 total, distributed over 10 seconds) and from models of Type-II supernovae. Allowing axions to be produced from neutron-neutron bremsstrahlung in the core collapse, i.e. $NN \to NNa$ would have provided a free-streaming energy loss channel for axion masses between roughly 0.001 and 1 eV, which would have foreshortened the neutrino pulse unacceptably.

The axion-photon coupling constant is directly constrained by horizontal branch (HB) stars to be $g_{a\gamma\gamma} < 10^{-10}$ GeV^{-1}[14]. This bound derives from the effect of axions produced by the Primakoff process in the nuclear

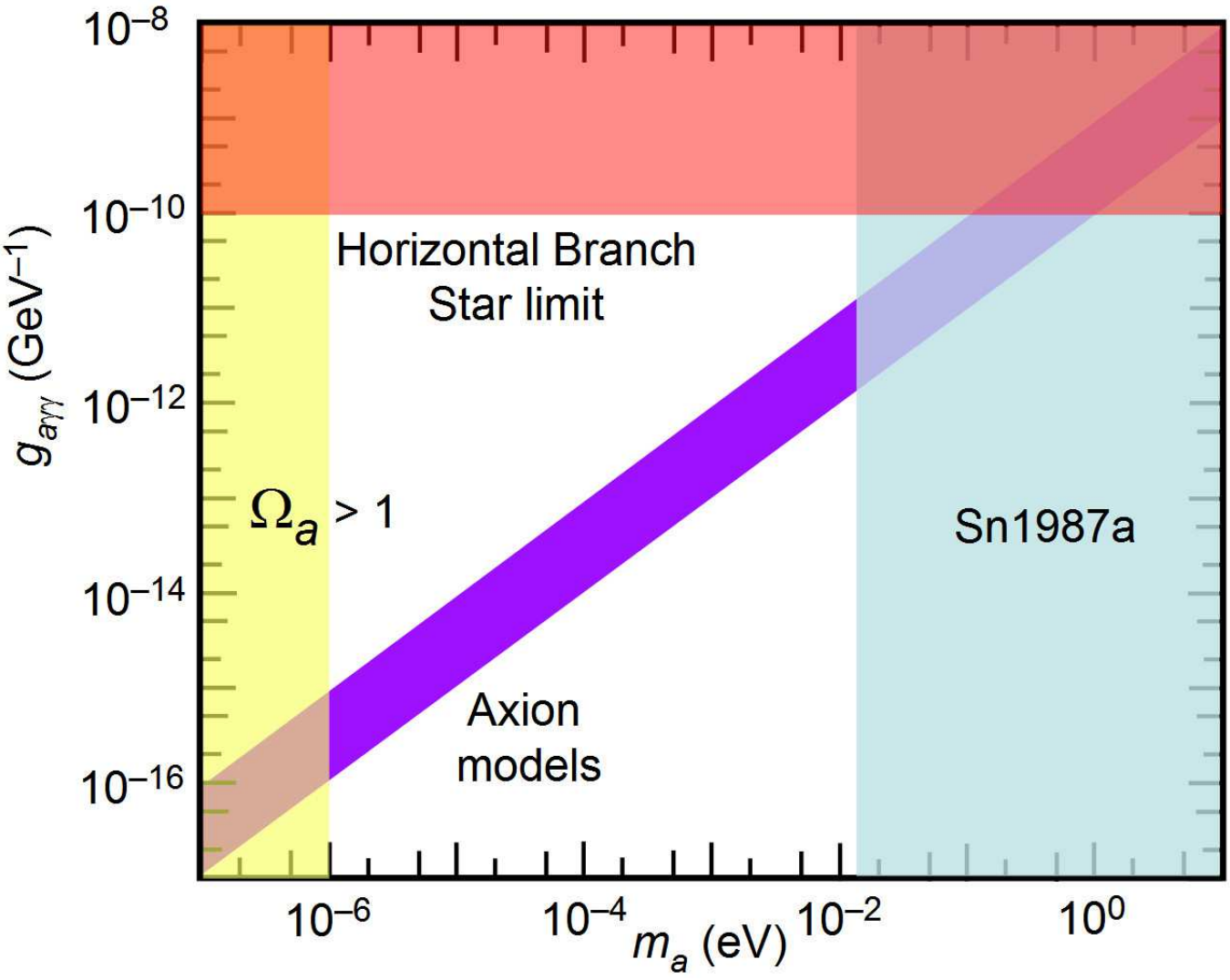

FIG. 1: Constraints on the axion mass m_a, and its coupling to two photons $g_{a\gamma\gamma}$ from cosmology and astrophysics, along with approximate representation of the band of theoretical models.

burning core, i.e. $\gamma + Ze \to a + Ze$, again representing a free-streaming energy loss channel which would disrupt the agreement of stellar evolution models with observational systematics of cohort star populations.

Coupled with other stellar bounds and previous laboratory experiments, all standard axions of mass $m_a > 10^{-3}$ eV are excluded. Assuming axions to be the dark matter of our galactic halo, the ADMX microwave cavity experiment has excluded KSVZ axions within the narrow range $1.9 < m_a < 3.3$ μeV; earlier searches set limits up to 16 μeV although for considerably stronger couplings[15]. The CAST experiment searching for solar axions set limits on $g_{a\gamma\gamma}$ approximately equal to the HB star limit[16]. The cosmological and astrophysical limits on the axion, and an approximate representation of the theoretical models (m_a vs. $g_{a\gamma\gamma}$) are shown in Fig. 1.

III. RESONANTLY ENHANCED PHOTON REGENERATION

The action density for the dynamics of photons and axions is

$$\begin{aligned} \mathcal{L} &= \frac{1}{2}(\epsilon E^2 - B^2) + \frac{1}{2}(\partial_t a)^2 \\ &- \frac{1}{2}(\vec{\nabla} a)^2 - \frac{1}{2} m_a^2 a^2 - g_{a\gamma\gamma} a \vec{E} \cdot \vec{B}, \end{aligned} \tag{5}$$

where $\vec{E}$, $\vec{B}$ and a are respectively the electric, magnetic and axion fields. The electromagnetic fields are given in terms of scalar and vector potentials, $\vec{E} = -\vec{\nabla}\Phi - \partial_t\vec{A}$, $\vec{B} = \vec{\nabla}\times\vec{A}$, as usual. The dielectric function ϵ is assumed constant in both space and time. In the presence of a large static magnetic field $\vec{B}_0(\vec{x})$, the equations of motion are

$$\begin{aligned} \epsilon\vec{\nabla}\cdot\vec{E} &= g_{a\gamma\gamma}\vec{B}_0\cdot\vec{\nabla}a \\ \vec{\nabla}\times\vec{B} - \epsilon\partial_t\vec{E} &= -g_{a\gamma\gamma}\vec{B}_0\partial_t a \\ \partial_t^2 a - \vec{\nabla}^2 a + m_a^2 a &= -g_{a\gamma\gamma}\vec{E}\cdot\vec{B}_0. \end{aligned} \tag{6}$$

$\vec{B}$ now represents the magnetic field minus $\vec{B}_0$, and terms of order $g_{a\gamma\gamma}aE$ and $g_{a\gamma\gamma}aB$ are neglected. Eqs. (6) describe the conversion of axions to photons and vice-versa.

Using these equations, it can be shown[3,4,17] that the photon to axion conversion probability P in a region of length L, permeated by a constant magnetic field B_0 transverse to the direction of propagation, is given by ($\hbar = c = 1$)

$$P = \frac{1}{4}\frac{1}{\beta_a\sqrt{\epsilon}}\left(g_{a\gamma\gamma}B_0 L\right)^2\left(\frac{2}{qL}\sin\frac{qL}{2}\right)^2, \tag{7}$$

where β_a is the axion speed and $q = k_a - k_\gamma$ is the momentum transfer. In terms of the energy ω, which is the same for the axion and the photon, $k_a = \sqrt{\omega^2 - m_a^2}$, $\beta_a = k_a/\omega$ and $k_\gamma = \sqrt{\epsilon}\omega$. The axion to photon conversion probability in this same region is also equal to P. Everything else being the same, the conversion probability is largest when $q \approx 0$. For $m_a << \omega$, and propagation in a vacuum ($\epsilon = 1$),

$$q = -\frac{m_a^2}{2\omega}. \tag{8}$$

Fig. 2a shows the photon regeneration experiment as usually conceived. If E_0 is the amplitude of the laser field propagating to the right, the amplitude of the axion field traversing the wall is $E_0\sqrt{P}$ where P is the conversion probability in the magnet on the LHS of Fig. 1a. Let P' be the conversion probability in the magnet on the RHS. The field generated on that side is then $E_S = E_0\sqrt{P'P}$ and the number of regenerated photons is $N_S = P'PN_0$ where N_0 is the number of photons in the initial laser beam.

Fig. 2b shows the two improvements[5,6] we propose for the experiment. The first is to build up the electric field on the left hand side of the experiment using a Fabry-Perot cavity, as illustrated. We will call this cavity the axion generation cavity. Assuming an amplitude transmissivity of t_{1a} of the input mirror, amplitude reflectivities of the two cavity mirrors r_{1a} and $r_{2a} \approx 1$, and a cavity length such that the multiple reflections between the mirrors interfere constructively, then the right-propagating field inside the cavity, E_a, will be:

$$E_a = \frac{2t_{1a}}{t_{1a}^2 + V_a}E_{in} \tag{9}$$

where E_{in} is the amplitude of the laser field going into the cavity and V_a is the fractional power loss the light encounters during one round-trip inside the cavity, less the losses due to the transmissivity of the input mirror. Hence, V_a includes power absorption in both mirrors, scattering due to mirror defects, diffraction from the finite mirror size, and the (small) leakage through mirror 2. The circulating light in the cavity creates an axion field of amplitude

$$a = \sqrt{P}E_a = \sqrt{P}\frac{2t_{1a}}{t_{1a}^2 + V_a}E_{in} \tag{10}$$

As long as $\omega \gg m_a$, the spatial distribution of the axion field is identical to the spatial distribution of the electric field. Assuming the lasers in Fig. 1a and Fig. 1b have the same power, the flux is increased by the factor $4t_a^2/(t_{1a}^2 + V_a)^2$ compared to the case without generation cavity. These axions propagate through the "wall" and reconvert into photons in the regeneration region.

As we have said, increasing the axion production rate, and thus the photon regeneration rate, by building up the optical power in the first magnet is not a new idea. In fact, the very first photon regeneration experiment performed and published by the BFRT collaboration[18,19] utilized an "optical delay line," which caused the laser beam to traverse the magnet 200 times before exiting. With relatively modest magnets (4.4 m, 3.7 T each), a limit of $g_{a\gamma\gamma} < 6.7\times10^{-7}$ GeV^{-1} was set. Four more photon-regeneration results have recently been reported. The BMV collaboration utilized a short, pulsed high-field magnet (0.37 m, 12.3 T), and pulsed laser fields ($\omega = 1.17$ eV, 1.5 kJ/pulse, 4.8 ns, firing every 2 hours), reaching a limit of $g_{a\gamma\gamma} < 1.25\times10^{-6}$ GeV^{-1} [20]. The GammeV collaboration built upon a single Tevatron dipole (6m, 5T) with a movable optical barrier in the middle to divide the magnet into production and regeneration regions, was the most sensitive, setting an upper bound to the axion-photon coupling of

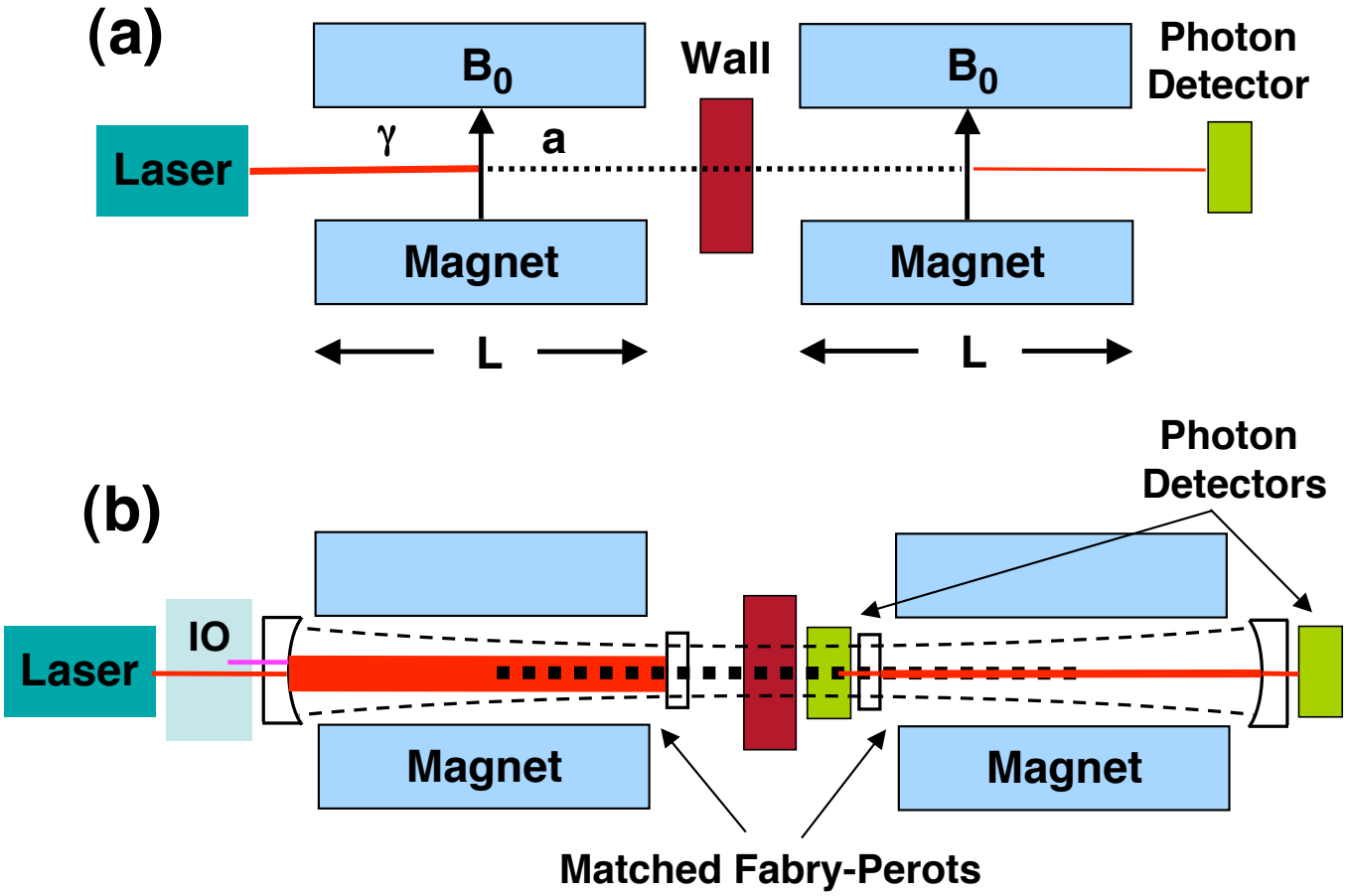

FIG. 2: (a) Simple photon regeneration. (b) Resonant photon regeneration, employing matched Fabry-Perot cavities. The overall envelope schematically shown by the thin dashed lines indicates the important condition that the axion wave, and thus the Fabry-Perot mode, in the photon regeneration cavity must follow that of the hypothetically unimpeded photon wave from the Fabry-Perot mode in the axion generation magnet. Between the laser and the cavity is the injection optics (IO) which manages mode matching of the laser to the cavity, imposes RF sidebands for reflection locking of the laser to the cavity, and provides isolation for the laser. The photon detectors are also preceded by matching and beam-steering optics. Layout is only schematic; as will be seen later, IO will likely be placed between the cavities.

$g_{a\gamma\gamma} < 3.5 \times 10^{-7}$ GeV^{-1} [21]. The LIPSS[22] collaboration used a pulsed free electron laser and two identical magnets (1.77 T, 1 m) and reached a limit similar to the BMV limit. Also the OSQAR experiment[23] reached a similar upper limit using a 18 W argon laser and one LHC dipole magnet (9.5 T, 14.3 m)separated into two halves by an optical barrier. These limits are valid only for axion masses below about one meV, with the full sensitivity of the BMV experiment extending to $m_a \approx 2$ meV, due to the shorter length of the magnet; see Figure 3. Other experiments are in various stages of preparation[24].

There is substantial gain from building up the laser power in the axion production magnet; however, it is immaterial whether one "recycles" the photons incoherently, as in an optical delay line, or coherently, as in a Fabry-Perot cavity. In contrast, the coherent case alone can provide a large additional gain in sensitivity for photon regeneration. Thus, the second improvement[5,6] is to install also a second Fabry-Perot cavity, the photon regeneration cavity, on the other side of the experiment, making a symmetric arrangement, as illustrated on the right-hand side of Fig. 2b. In this setup, the axion field acts as a source field similar to a gain medium in a laser resonator. The intra-cavity field can be calculated using the equilibrium condition:

$$E_\gamma = \frac{1}{1 - r_{1\gamma} r_{2\gamma} e^{i\phi_{RT}}} \eta \sqrt{P} a e^{ik_a d} \tag{11}$$

where ϕ_{RT} is the round trip phase of the field, d is the distance between the two cavities and $r_{1\gamma}$ and $r_{2\gamma}$ are the amplitude reflectivities of the two cavity mirrors. η is the spatial overlap integral between the axion mode and the electric field mode. This overlap will be identical to unity (up to corrections of order m_a/ω_0) if the spatial eigenmodes

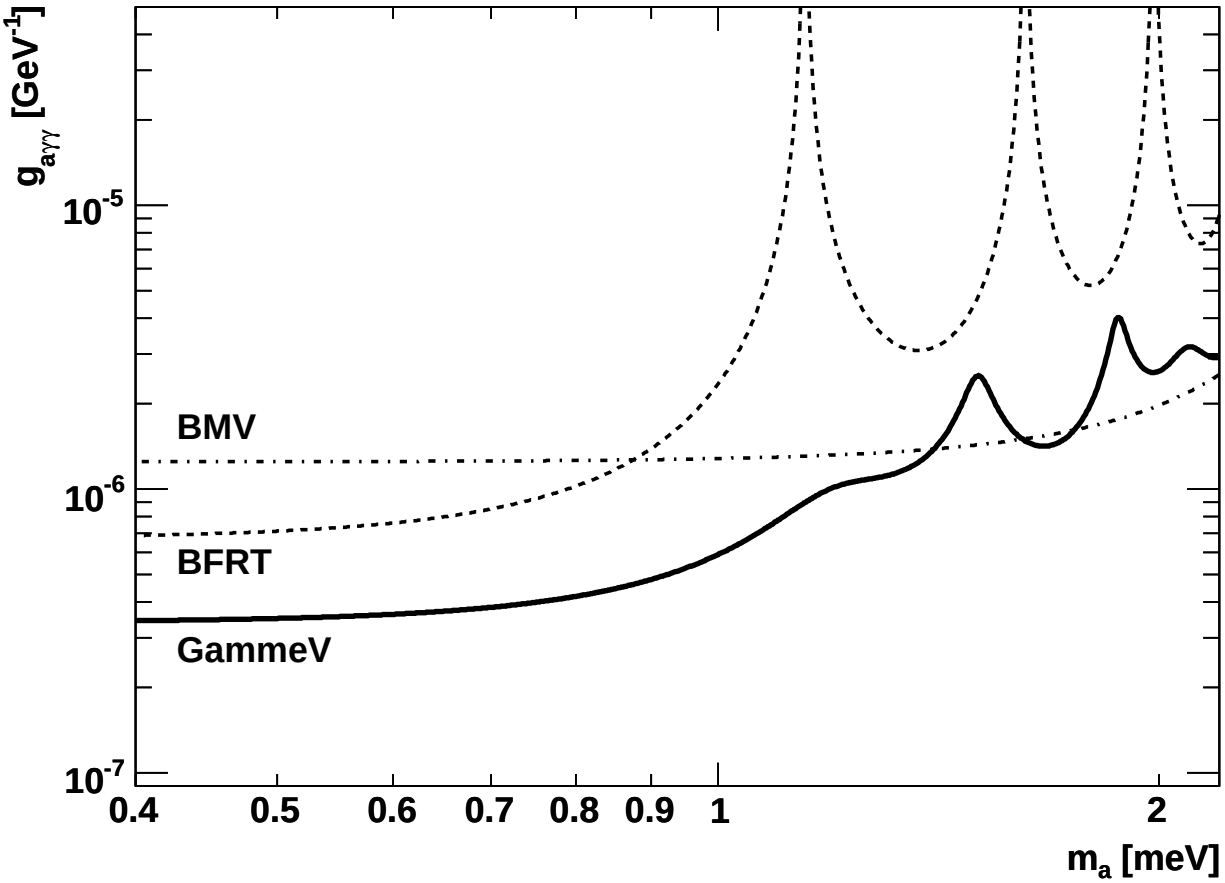

FIG. 3: Exclusion region from three photon-regeneration experiments reported to date.[18,19,20,21] See text for discussion.

of the two cavities are extensions of each other, e.g. when the Gaussian eigenmode in one cavity propagated to the other cavity is identical to the Gaussian eigenmode of that cavity.

The field will be resonantly enhanced if $\phi_{RT} = N2\pi$. To detect the regenerated field, a small part is allowed to transmit through one of the cavity mirrors, say mirror 1, with an amplitude transmissivity of $t_{1\gamma}$:

$$E_S = t_{1\gamma} E_\gamma \approx \frac{2t_{1\gamma}}{t_{1\gamma}^2 + V_\gamma} \eta \sqrt{P} a e^{ik_a d} \tag{12}$$

Here we replaced the amplitude reflectivities with the amplitude transmissivities and intensity losses of the mirrors:

$$\begin{aligned} r_{1\gamma} &= \sqrt{1 - t_{1\gamma}^2 - V_{1\gamma}} \approx 1 - \frac{t_{1\gamma}^2}{2} - \frac{V_{1\gamma}}{2} \\ r_{2\gamma} &= \sqrt{1 - V_{2\gamma}} \approx 1 - \frac{V_{2\gamma}}{2} \qquad V_\gamma \equiv V_{1\gamma} + V_{2\gamma} \end{aligned} \tag{13}$$

The final regenerated electric field is:

$$\begin{aligned} E_S &= \left(\frac{2t_{1\gamma}}{t_{1\gamma}^2 + V_\gamma} \right) \eta P E_a e^{ik_a d} \\ &= \left(\frac{2t_{1\gamma}}{t_{1\gamma}^2 + V_\gamma} \right) \left(\frac{2t_{1a}}{t_{1a}^2 + V_a} \right) \eta P E_{in} e^{ik_a d} \end{aligned} \tag{14}$$

Or in terms of regenerated photons:

$$N_S = \left(\frac{4T_{1\gamma}}{(T_{1\gamma}+V_\gamma)^2}\right)\left(\frac{4T_{1a}}{(T_{1a}+V_a)^2}\right)\eta^2 P^2 N_{in} \tag{15}$$

where we have replaced the amplitude transmissivities with the commonly used intensity or power transmissivities $T = |t|^2$.

The final signal depends on the laser power build-up in the axion generation cavity and the signal build-up in the photon regeneration cavity. The build-up in the regeneration cavity is only limited by the losses V_γ and the transmissivity $T_{1\gamma}$. As always, the field outside the cavity is maximum when the cavity is impedance matched ($T = V$). The losses include coating absorption and scattering from imperfections in the polished surface, mainly small angle scattering. Current state-of-the-art mirrors have coating absorption of < 1 ppm and scatter of < 5 ppm or total losses in the order of $V \approx 10$ ppm for both mirrors combined. For the impedance-matched case, it is convenient to express Eq. (15) in terms of the finesse $\mathcal{F}_{\gamma,a}$ of the cavities:

$$N_S = \eta^2 \frac{\mathcal{F}_\gamma}{\pi}\frac{\mathcal{F}_a}{\pi} P^2 N_{in} \tag{16}$$

Note that resonant regeneration gives an enhancement factor of $\sim (\mathcal{F}/\pi)^2$ over simple photon regeneration. This factor may feasibly be 10^{10}, corresponding to an improvement in sensitivity to $g_{a\gamma\gamma}$ of ≈ 300.

The power build up in the axion generation cavity is further limited by thermal heating of the mirror surfaces caused by the absorption of the stored light in the mirror coatings. This heating will change the radii of curvature of the cavity mirrors, increase the scatter losses due to non-spherical higher order figure distortions, and create a thermal lens in the substrate of the input mirror[25]. Current estimates based on Ref.[25] suggest that we can operate the cavity with approximately 100 kW intra-cavity power without a dedicated thermal correction system. This value could be increased by at least one order of magnitude using a LIGO-like thermal correction system, mirror substrates with a higher thermal conductivity then fused silica such as sapphire, and/or cooling the mirrors to lower temperatures where there is a significant increase in the thermal conductivity of the mirror substrates[26]. The axion generation cavity can potentially increase the number of generated axions by 5 orders of magnitude while the photon regeneration cavity potentially increases the number of regenerated photons by another 5 orders of magnitude.

IV. EXPERIMENTAL IMPLEMENTATION

The resonantly-enhanced photon regeneration experiment, involving the design and active locking of high-finesse Fabry-Perot resonators and the heterodyne detection of weak signals at the shot-noise limit, is well supported by the laser and optics technology developed for LIGO[7]. This section will discuss all aspects of the experimental implementation while the next section will present estimates of the achievable experimental sensitivity for a realistic design in terms of power-handling capabilities and mirror technologies.

A. Magnets

The design utilizes a total of 12 Tevatron superconducting dipoles (each 5T field, 6m length, and 48mm diameter warm bore), 6 for the axion generation cavity and 6 for the photon regeneration cavity; hereafter referred to as the "TeV 6+6" configuration. There is a large infrastructure and experience base for the Tevatron dipoles, and an adequate number are available.

B. Cavity design

The layout requires that the optical cavities are mode-matched to each other. In addition, losses due to aperture effects should be kept very low. These considerations, together with the dimensions of the available magnets, drive the design of the two optical cavities. The waist of the optical eigenmode of both cavities should be half way between the cavities, at or near the location of the beam block. The magnets plus the necessary space between each magnet and at the ends of the magnets set the final length of each cavity. Although all details have not yet been worked out, we expect that the end mirror of each cavity will be about 46 m away from the waist. The central mirrors can be placed within 2 m of each other or 1 m away from the waist implying a cavity length of $L_{cav} = 45$ m.

Although Fig. 2 schematically shows the laser light being fed to the axion generation cavity at the far end (relative to the waist) it is clearly preferable to inject the light in the space between the mirrors. This approach minimizes the separation of the injection/locking circuits from the optics and electronics that lock the photon regeneration cavity. (See discussion below.) The rest of the paper uses this approach as the baseline.

The free spectral range of each cavity would then be:

$$FSR = \frac{c}{2 \times L_{cav}} \approx 3.3\,\mathrm{MHz} \tag{17}$$

The optical cavities have to support mirror-image fundamental spatial modes and should suppress all higher order spatial modes. Therefore, we choose g-parameters[27] for the optical cavities such that $g_1 g_2 = 0.6$, where $g_i = 1 - L_{cav}/R_i$, with R_i the radii of curvature of the mirrors. The transversal mode spacing is then:

$$\Delta\nu_{TEM} = \frac{\mathrm{acos}(\sqrt{g_1 g_2})}{\pi} \times FSR \approx 726\,\mathrm{kHz} \tag{18}$$

Using the dependence of the mirror locations with respect to the waist of the eigenmode on the g-factors and the length of the cavity[27],

$$\begin{aligned} z_1 &= \frac{g_2(1-g_1)}{g_1+g_2-2g_1g_2} L_{cav} = -1\,\mathrm{m} \\ z_2 &= \frac{g_1(1-g_2)}{g_1+g_2-2g_1g_2} L_{cav} = 46\,\mathrm{m} \end{aligned} \tag{19}$$

we can calculate the individual g-factors:

$$g_1 = 1.015 \qquad g_2 = 0.591. \tag{20}$$

The beam sizes w_i on the mirrors and the waist w_0 are then:

$$w_1 = 4.29\,\mathrm{mm} \approx w_0 \qquad w_2 = 5.62\,\mathrm{mm} \tag{21}$$

The beam size at the input mirror is essentially identical to the waist size. The mirror radii of curvatures are nominally:

$$\begin{aligned} ROC_1 &= \frac{L_{cav}}{1-g_1} = -2946\,\mathrm{m} \approx \infty \\ ROC_2 &= \frac{L_{cav}}{1-g_2} = 110\,\mathrm{m}. \end{aligned} \tag{22}$$

If we replace the input mirror by a flat mirror, the loss from mode mismatch between the two cavities is less than 10^{-4} in field amplitude while the beam sizes would increase by $\sim 10\,\mu$m. For all practical purposes, it is sufficient to assume a flat input mirror. Note that the intensity on the mirror in the center of the beam for an intra-cavity power of 1 MW would be:

$$I = 2\frac{P}{\pi w^2} \approx 3.5 \frac{\mathrm{MW}}{\mathrm{cm}^2} \frac{P_{cav}}{[1\,\mathrm{MW}]} \tag{23}$$

well below the damage threshold of modern coatings.

The Tevatron magnets have a 48 mm cold bore and are slightly curved. They will be attached to each other such that the clear aperture wiggles around the optical axis but possesses no net bend over all 12 magnets. We estimated that the clear aperture through the entire 12 magnets will be ~ 39 mm well beyond the necessary aperture given the above derived beam sizes. However, clipping at the aperture of the Tevatron magnets could limit future expansions of the experiment to about 100 m length for each cavity.

In addition to mode mismatch because of mismatched beam sizes and radii of curvatures, the efficiency of photon regeneration will also depend on alignment mismatches between the cavities. Angular or lateral misalignment of the optical axes would significantly reduce the spatial overlap between the two modes. Losses caused by a lateral shift δx scale with the beam size, those caused by an angular shift scale with the divergence angle, so that the overall efficiency is:

$$\eta \approx 1 - \frac{1}{2}\frac{\delta x^2}{w_1^2} - \frac{1}{2}\frac{\delta\alpha^2}{\Theta^2} \qquad \text{with :} \qquad \Theta = \frac{\lambda}{\pi w_1} \tag{24}$$

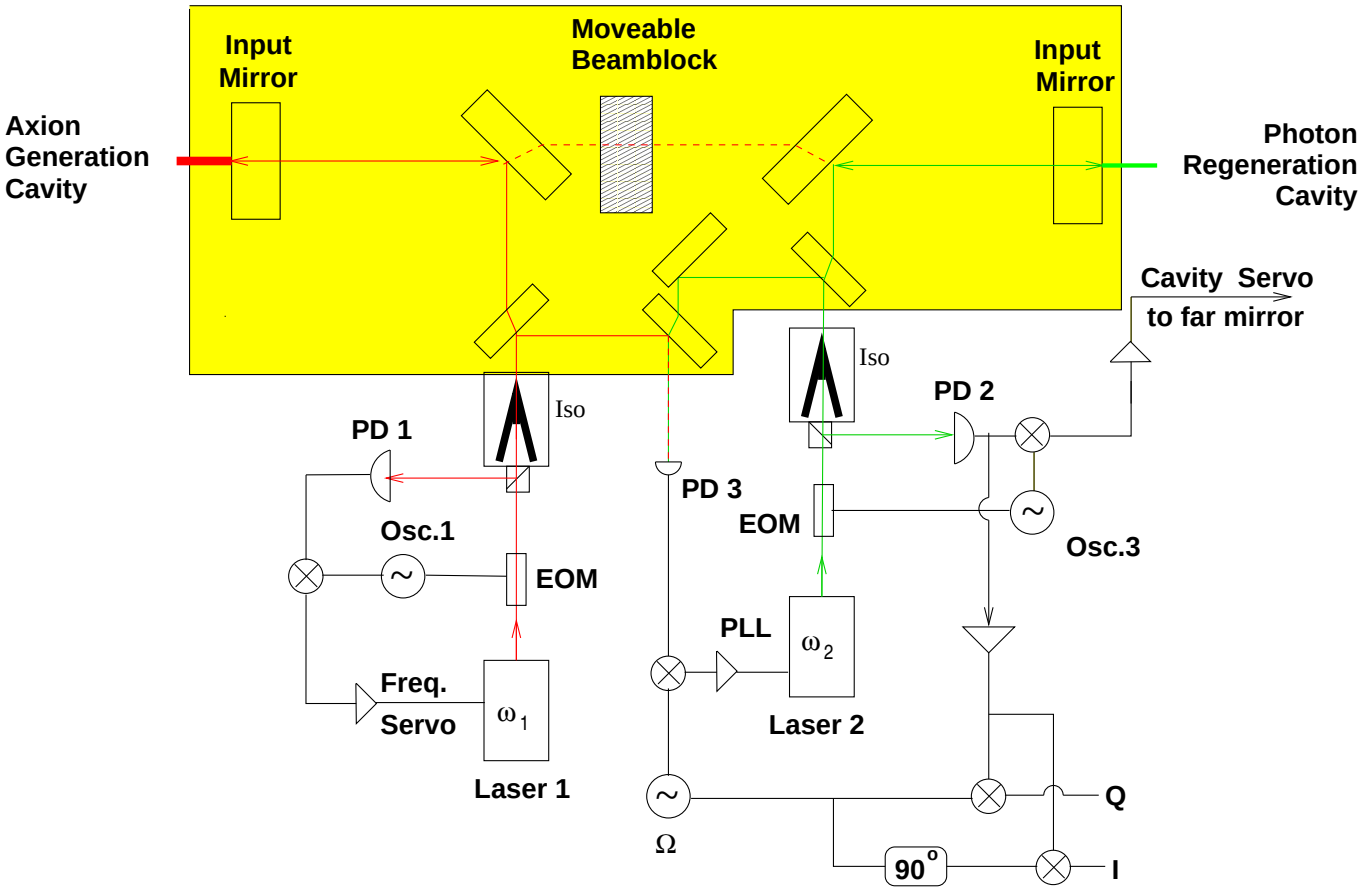

FIG. 4: Schematic of the Pound-Drever-Hall stabilization and locking technique of the two cavities, and the heterodyne demodulation scheme for detection of the signal. EOM: Electro-optical Modulator PLL: Phase Lock Loop, Iso: Optical Isolator, PD: Photo detector. The red dashed line indicates the beam line of the leakage field from the Axion generation cavity. After removing the beam block, this beam can be used to align both cavities.

Recall that η is the spatial overlap integral between the axion mode and the electric field mode. Requiring an efficiency $\eta > 0.95$, the requirements on the lateral and angular offsets for the proposed TeV 6+6 configuration are:

$$\delta x < \sqrt{0.05} w_1 \approx 1\,\mathrm{mm}; \tag{25}$$

$$\delta\alpha < \sqrt{0.05}\Theta \approx 17\,\mu\mathrm{rad}, \tag{26}$$

This alignment has to be checked periodically as part of the run protocol.

C. Length and frequency stabilization system

Intrinsic to resonantly enhanced photon regeneration is the requirement that the axion generation and photon regeneration cavities are both on resonance with the axion generating laser field E_{in}. The proposed experimental setup to achieve these conditions is shown in Figure 4. The laser frequency ω_1 of Laser 1 which resonates inside the axion generation cavity will be stabilized to the eigenfrequency of the cavity by means of a modulation/demodulation technique commonly known as the Pound-Drever-Hall technique[28]. In this technique, the phase of the laser field is modulated with an electro-optic modulator (EOM) before it enters the cavity. This modulation creates a pair of sidebands offset from the carrier by $\pm$ the modulation frequency. These sidebands are not resonant inside the cavity and are directly reflected at the front mirror of the optical cavity while the carrier enters the cavity. The cavity internal carrier field then transmits back out through the front mirror, where it is superimposed on the directly reflected carrier field. If the carrier is on resonance in the optical cavity, its round-trip phase shift is a multiple of 2π

and the leakage field is π out of phase with the directly reflected component. Consequently, the superposition between carrier and sidebands maintains its phase modulation character, *i.e.*, the generated photocurrent does not show any modulation at the phase modulation frequency. If the carrier is slightly off resonance in the optical cavity, its round trip phase shift is not exactly a multiple of 2π, and the superposition between carrier and sidebands can no longer be described as a pure phase modulation but includes now also some amplitude modulation. The amplitude modulation is directly proportional to the round trip phase shift (modulo 2π) or the frequency offset between the carrier field and the resonance frequency of the cavity. Moreover, it changes sign as the cavity passes through resonance. This signal is detected, amplified, filtered and fed back to the laser's frequency actuators.

Axions regenerated as photons in the photon regeneration cavity will have the same frequency as the laser photons. Thus, resonant photon regeneration requires that an eigenfrequency of this cavity must be well within the linewidth of the resonance of the axion generation cavity. This resonance condition may be achieved and maintained by means of Laser 2 of frequency ω_2 that is offset from the frequency of Laser 1. Light from Laser 2 will first be mixed with some light picked off from Laser 1; the beat signal will be demodulated with a tunable RF frequency. The demodulated signal will then be amplified and filtered before it is fed back to the frequency actuators of the Laser 2 to maintain a heterodyne phase lock between the two lasers. The difference frequency is then identical to the RF frequency $\Omega = \omega_1 - \omega_2$, which will be set to equal a multiple of the free spectral range of the photon regeneration cavity. The field from Laser 2 is then injected into the photon regeneration cavity and one of the eigenfrequencies of this cavity is then locked to the frequency of Laser 2 using again the Pound-Drever-Hall scheme described above, the sole difference being that here the feedback controls the length of the second cavity (through piezo transducers acting on one of the mirrors), rather than controlling the laser frequency as is done in the axion generation cavity.

Heterodyne detection of the signal

The axion field will coherently generate a signal field E_S at laser frequeny ω_1 with a phase which depends on the geometric distance between the two cavities. After leaving the photon regeneration cavity, this field has the form (see equation 12):

$$E_S = E_{SO} e^{i\omega_1 t} e^{i\phi} \qquad \phi = k_a d \tag{27}$$

This field, mode matched to the photon regeneration cavity, will propagate towards the photodetector which is also used to generate the Pound-Drever-Hall signal for the cavity stabilization. In addition, the field from Laser 2 is used as the local oscillator for the signal field. The photodiode signal is the beat between the two fields, given by:

$$\begin{aligned} S &= \left| E_{SO} e^{i(\omega_1 t + \phi)} + E_{LO} e^{i\omega_2 t} \right|^2 \\ &= E_{LO}^2 + 2 E_{LO} E_{SO} \cos(\Omega t + \phi) \end{aligned} \tag{28}$$

where we have assumed that $E_{SO} \ll E_{LO}$. The limiting noise source in the detection process will be shot noise. Therefore, it is convenient to express the signal in terms of the number of photons in both fields:

$$S = N_{LO} + S_I \cos\Omega t - S_Q \sin\Omega t \tag{29}$$

where:

$$S_I = 2\sqrt{N_{LO} N_S} \cos\phi \qquad S_Q = 2\sqrt{N_{LO} N_S} \sin\phi \tag{30}$$

are the two quadrature components of the signal.

The shot noise or variance in each quadrature can be calculated from the number of photons detected:

$$\sigma_I = \sqrt{2\bar{N}} = \sqrt{2N_{LO}} = \sigma_Q. \tag{31}$$

The factor $\sqrt{2}$ is a fundamental consequence of the detection process. The local oscillator beats with the vacuum fluctuations at frequency $\omega_0 + \Omega$ and at $\omega_0 - \Omega$ to generate a beat signal at Ω. These two contributions are statistically independent and add quadratically. The signal to shot noise ratio is then:

$$\frac{S_I}{\sigma_I} = \sqrt{2N_S} \cos\phi; \qquad \frac{S_Q}{\sigma_Q} = \sqrt{2N_S} \sin\phi. \tag{32}$$

If we could adjust the phase to guarantee that $\phi \ll 1$ all the time, our signal to noise in the in-phase quadrature would be $\sqrt{2N_S}$. This phase includes for example the distance traversed by the axion field, which is not commensurate with

the other optical paths. Therefore, it is currently not clear how to adjust this phase. Instead, it is likely that our starting phase during the detection process is arbitrary and that we have to combine both quadratures to measure the amplitude in the signal:

$$S_\Sigma = \sqrt{S_I^2 + S_Q^2} = 2\sqrt{N_{LO} N_S}. \tag{33}$$

Similarly, the shot noise in both quadratures adds quadratically:

$$\sigma_\Sigma = \sqrt{\sigma_I^2 + \sigma_Q^2} = 2\sqrt{N_{LO}} \tag{34}$$

and the signal to shot noise is:

$$\frac{S_\Sigma}{\sigma_\Sigma} = \sqrt{N_S}, \tag{35}$$

where N_S is the number of regenerated photons in the signal field. As expected, to obtain a signal to noise ratio of one requires one detected photon.

Using equation 7, assuming $qL/2 \ll 1$, and impedance matched cavities ($T_1 \approx V$), the number of regenerated photons can be approximated as follows:

$$\begin{aligned} N_S &= \eta^2 \frac{\mathcal{F}_\gamma}{\pi} \frac{\mathcal{F}_a}{\pi} \frac{1}{16} (g B_0 L)^4 N_{in} \\ &= \eta^2 \frac{\mathcal{F}_\gamma}{\pi} \frac{\mathcal{F}_a}{\pi} \frac{1}{16} (g B_0 L)^4 \frac{P_{in}}{\hbar \omega_0} \tau \end{aligned} \tag{36}$$

where τ is the measurement time and P_{in} is the power of the first laser coupled into the axion generation cavity. During this measurement time the standard deviation in the number of detected photons increases with $\sqrt{\tau}$. Consequently, the signal to shot noise increases as $\sqrt{\tau}$.

D. Noise sources and Efficiencies

So far, this analysis assumes that the phase ϕ is constant. Changes in the detection phase can be understood as phase modulation of the signal:

$$\begin{aligned} \phi(t) &= <\phi(t)>_T + \delta\phi(t) \\ &= \phi_0 + \frac{1}{\sqrt{2\pi}} \int_{-\infty}^{\infty} \tilde{\phi}(f) e^{i2\pi f t} df \\ e^{i(\omega_0 t + \phi)} &\approx e^{i(\omega_0 t + \phi_0)} \left[1 + \frac{i}{\sqrt{2\pi}} \int_{\infty}^{\infty} \tilde{\phi}(f) e^{i2\pi f t} df \right] \end{aligned} \tag{37}$$

where $\tilde{\phi}(f)$ is the linear spectral density of the phase fluctuations. This modulation shifts power into other frequency components and reduce the main signal. Consequently, the amplitude of the phase modulation has to be sufficiently small. This condition is roughly equivalent to requesting that the rms-phase fluctuations stay below about 1 rad:

$$\delta\phi_{rms} = \sqrt{\int_{1/T}^{\infty} \tilde{\phi}^2(f) df} < 1\,\text{rad} \tag{38}$$

Note that this phase is the differential phase between the two laser fields, which is controlled by a heterodyne phase-locked loop. The reference signal for this phase-locked loop is also used to demodulate the signal itself. Sources for potential phase changes are changes in the distance between the two cavities, differential changes in the distance between BS_1 and BS_2 and between BS_1 and the axion generation cavity, and changes in the phase of the reference signal. A satisfactory solution could be to mount all optical components on a breadboard made from a material with a very low coefficient of thermal expansion such as a Zerodur or ULE and temperature stabilize the entire breadboard to keep the geometric and optical distances stable. Large variations in the phase of the reference signal are not expected, as this is a radio frequency phase and typical cable lengths are shorter than the wavelength of the RF signal. Length changes of the photon regeneration cavity will in first order change the phase of both fields by the same amount. Note

that the axion generation cavity is the reference length of the entire experiment and any changes in it will be tracked by the laser fields.

Not every photon which reaches the active area of the photodetector will generate an electron. Some photons will be reflected; others will excite electron-hole pairs which recombine in the active area. These effects reduce the efficiency of the photodetector. Typical quantum efficiencies of commercial photodetectors are on the order of 80% but several InGaAs detectors have reached quantum efficiencies of 95%[29].

One technical noise source that needs to be considered is the dark current of the photodetector. This is usually measured in terms of noise equivalent power (NEP) per root Hz (or equivalently the noise at the measurement frequency integrated over a measurement time of one second). The beat frequency is equal to the free spectral range of the cavity which is approximately 3.3 MHz for a 45 m long cavity. Typical photodetectors with sufficient bandwidth have a noise equivalent power of less than 1 pW/$\sqrt{\text{Hz}}$ in the frequency range of interest, and saturate at an input power of a few mW. Assuming a power of the local laser of P_{LO} =1 mW, the shot noise would be:

$$\sigma = 15 \frac{\text{pW}}{\sqrt{\text{Hz}}} \tag{39}$$

well above the noise of the photodetector.

V. NUMERICAL EVALUATION AND DISCUSSION

For the example of the TeV 6+6 setup described above, an input power of 10 W, a cavity finesse of $\mathcal{F} \sim \pi \times 10^5$ ($T = 10\,\text{ppm} = V$) for both cavities, and a $SNR = 1$ we find

$$\begin{aligned} g_{a\gamma\gamma}^{min} &= \frac{2.0 \times 10^{-11}}{\text{GeV}} \left[\frac{0.95}{\eta}\right] \left[\frac{180\,\text{Tm}}{BL}\right] \left[\frac{10\,\text{ppm}}{T}\right]^{1/2} \\ &\times \left[\frac{10\,\text{W}}{P_{in}}\right]^{1/4} \left[\frac{10\,\text{days}}{\tau}\right]^{1/4} \end{aligned} \tag{40}$$

after 10 days of measurement time. This translates into a 95% exclusion limit (3σ) for axions or generalized pseudoscalars with $g_{a\gamma\gamma}^{min} < 2.0 \times 10^{-11}\text{GeV}^{-1}$after 90 days cumulative running, well into territory unexplored by stellar evolution bounds or direct solar searches. Note that the exclusion sensitivity follows the inverse of $\text{sinc}(qL/2)$, for the case of the TeV 6+6 configuration, the first null sensitivity occuring at 2.8×10^{-4}eV. The momentum mismatch between a massless photon and a massive axion defines the oscillation length of the process to be $L_{osc} = 2\pi/q$.

As pointed out in Ref.[4] however, there is a practical strategy to extend the mass range upwards if the total magnetic length L is comprised of a string of N individual identical dipoles of length l. In this case, one may configure the magnet string as a "wiggler" to cover higher regions of mass, up to values corresponding to the oscillation length determined by a single dipole, i.e. $q \sim l^{-1}$. The dotted boundaries in figure 4 depicts how the "wiggler" configurations can extend the mass reach of the exclusion regions; e.g. in the case of the TeV 6+6 setup, additional running in the combinations of magnet configurations ↑↑↑↑↑↑, ↑↑↑↓↓↓,, ↑↑↓↓↑↑ and ↑↓↑↓↑↓ extend the mass reach by a factor $\sqrt{6}$ up to $\sim 6 \times 10^{-4}$ eV.

Clearly the most efficient way to extend the discovery (or exclusion) potential of the experiment to lower values of $g_{a\gamma\gamma}$ is to make a longer and/or stronger magnetic string; $g_{a\gamma\gamma} \propto (BL)^{-1}$. While resonant photon regeneration marks a significant improvement over the simple experiment, in fact the sensitivity in $g_{a\gamma\gamma}$ still only gains (or loses) as $\mathcal{F}^{1/2}$. Thus in our example, the experiment would still reach a limit of $g_{a\gamma\gamma} = 6.2 \times 10^{-11}$ GeV^{-1} even if the Fabry-Perot only achieved a finesse of $\mathcal{F} \simeq 30,000$. Assuming 10 ppm intra cavity losses without diffraction, the optimum magnet length is reached when the aperture causes additional 5 ppm losses. For a clear aperture of 39 mm diameter, the optimum length would then be $L_{opt} \approx 90$ m and, assuming impedance matched cavities, an intra cavity power of 1 MW, and 5T-Tevatron magnets, $g_{a\gamma\gamma}^{min} \approx 8.7 \times 10^{-12}\text{GeV}^{-1}$. This limit can further be improved using straight Tevatron magnets with a clear aperture of 48 mm and an optimum length of ≈ 140 m to $g_{a\gamma\gamma}^{min} \approx 5.8 \times 10^{-12}\text{GeV}^{-1}$.

Thus without future dramatic improvements in superconducting magnet technology, the reach in sensitivity for resonantly-enhanced photon regeneration will likely fall short of the axion model band in parameter space by roughly two to three orders of magnitude at $m_a \sim 10^{-4}$ eV, and three to four orders of magnitude at $m_a \sim 10^{-5}$ eV. Presumably the microwave cavity experiments[3,15] will be able to cover the 10 μeV range with adequate sensitivity to find or exclude the axion, assuming that axions constitute the dominant component of the Milky Way halo dark matter. Of course, we have no *a priori* knowledge of the axion model found in nature or even if it is to be found at all, and thus one should be open to surprise once any new region of parameter space becomes accessible.

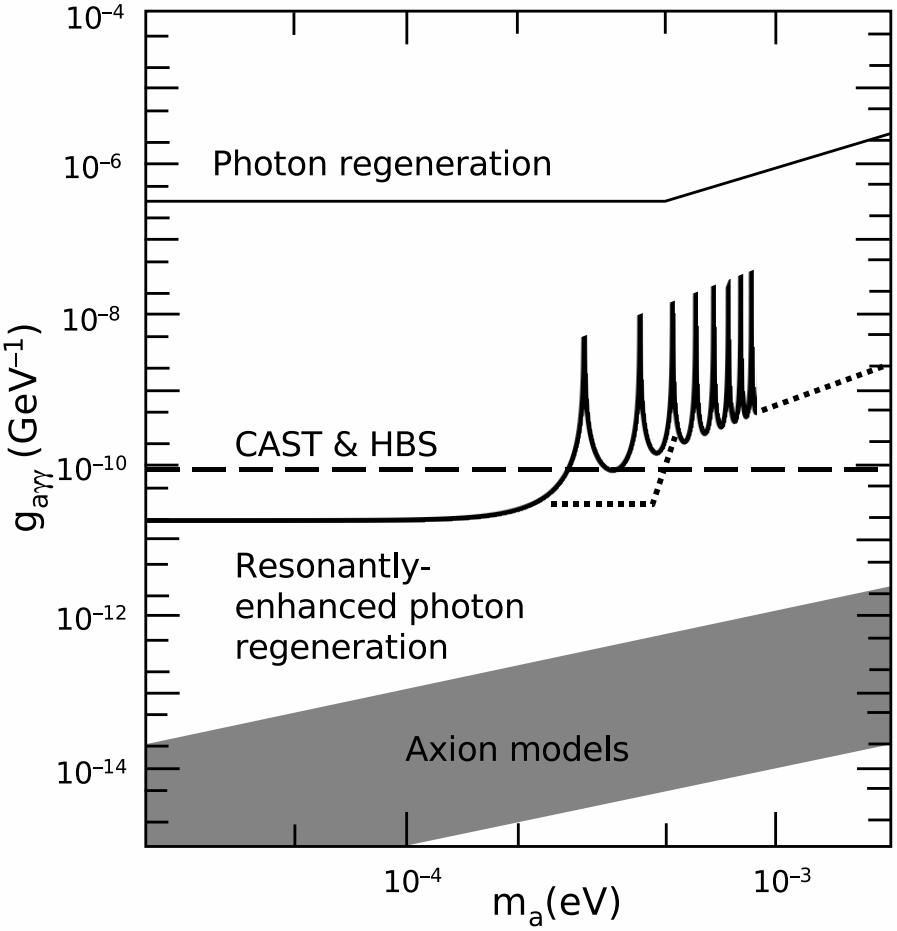

FIG. 5: Current exclusion plot of mass and photon coupling $(m_a, g_{a\gamma\gamma})$ for the axion, and the 95% CL exclusion limit for the resonantly enhanced photon regeneration experiment calculated for the TeV 6+6 configuration and with a cavity finesse of 3.1×10^5. The solid curve represents the exclusion region with all magnets of the same polarity; the dotted lines indicate the additional reach in mass by running in all "wiggler" configurations, as described in the text. The existing exclusion limits indicated on the plot include the best direct solar axion search (CAST collaboration)[16], the Horizontal Branch Star limit[14], and previous laser experiments.[18,19,20,21]

Acknowledgments

We thank Muzammil Arain, Tom Carruthers, Aaron Chou, Kem Cook, Bruce Macintosh, Frank Nezrick, Georg Raffelt, Dan Stancil, Ray Weiss, and Stan Whitcomb for useful conversations during the development of this concept. This work was supported in part under the auspices of the U.S. Department of Energy under contracts DE-FG02-97ER41029, and DE-AC52-07NA27344. P.S. gratefully acknowledges the hospitality of the Aspen Center of Physics while working on this project.

---

* Electronic address: mueller@phys.ufl.edu
† Also at Lawrence Livermore National Laboratory, Livermore, CA 94550, USA

[1] R. Bradley, John Clarke, Darin Kinion, Leslie J. Rosenberg, Karl van Bibber, Seishi Matsuki, Michael Mück, Rev. Mod. Phys. **75**, 777 (2003).
[2] P. Svrček and E. Witten, J. High Energy Phys. **0606**, 051 (2006).
[3] P. Sikivie, Phys. Rev. Lett. **51** 1415 (1983)

[4] K. van Bibber, N.R. Dagdeviren, S.E. Koonin, A.K. Kerman and H.N. Nelson, Phys. Rev. Lett. **59**, 759 (1987); for the case of exactly massless bosons, see A.A. Ansel'm, Yad. Fiz. **42**, 1480 (1985).

[5] Production and detection of light bosons using optical resonators. F. Hoogeveen, T. Ziegenhagen (Hannover U.). DESY-90-165, ITP-UH-5-1990, Nov 1990. 28pp. Published in Nucl. Phys. B **358**, 3 (1991).

[6] P. Sikivie, D.B. Tanner, and Karl van Bibber Phys. Rev. Lett. 98, 172002 (2007).

[7] B. Abbott et al.(LIGO Scientific Collaboration, Nucl. Instrum. Methods A **517** 154–179 (2004).

[8] R. D. Peccei and H. Quinn, Phys. Rev. Lett. **38**, 1440 (1977) and Phys. Rev. D **16**, 1791 (1977).

[9] S. Weinberg, Phys. Rev. Lett. **40**, 223 (1978); F. Wilczek, Phys. Rev. Lett. **40**, 279 (1978).

[10] M. Dine, W. Fischler and M. Srednicki, Phys. Lett. **104B**, 199 (1981); A. P. Zhitnitskii, Sov. J. Nucl. Phys. **31**, 260 (1980).

[11] J. Kim, Phys. Rev. Lett. **43**, 103 (1979); M. A. Shifman, A. I. Vainshtein and V. I. Zakharov, Nucl. Phys. B166, 493 (1980).

[12] L. Abbott and P. Sikivie, Phys. Lett. **120B**, 133 (1983); J. Preskill, M. Wise and F. Wilczek, Phys. Lett. **120B**, 127 (1983); M. Dine and W. Fischler, Phys. Lett. **120B**, 137 (1983).

[13] M. S. Turner, Phys. Rep. **197**, 67 (1990); G. G. Raffelt, Phys. Rep. **198**, 1 (1990).

[14] G.G. Raffelt, Stars as Laboratories for Fundamental Physics (University of Chicago Press, Chicago, 1996).

[15] S. Asztalos, L. Rosenberg, van K. Bibber, P. Sikivie, Konstantin Zioutas, Ann. Rev. of Nuc. Part. Sci. **56** 293-326 (2006).

[16] K. Zioutas et al. (CAST collaboration), Phys. Rev. Lett. **94**, 121301 (2005); E. Arik et al. (CAST collaboration) J. Cosmo. Astropart. Phys. (2009).

[17] G. Raffelt and L. Stodolsky, Phys. Rev. D **37**, 1237 (1988).

[18] G. Ruoso, R. Cameron, G. Cantatore, A. C. Melissinos, Y. Semertzidis, H. J. Halama, D. M. Lazarus, A. G. Prodell, F. Nezrick, C. Rizzo and E. Zavattini, Z. Phys. C **56**, 505 (1992).

[19] R. Cameron, G. Cantatore, A. C. Melissinos, G. Ruoso, and Y. Semertzidis, H. J. Halama, D. M. Lazarus, and A. G. Prodell, F. Nezrick, C. Rizzo and E. Zavattini, Phys. Rev. D **47**, 3707 (1993).

[20] C. Robilliard, R. Battesti, M. Fouch, J. Mauchain, A.-M. Sautivet, F. Amiranoff, and C. Rizzo, Phys. Rev. Lett. **99** 190403(4) (2007).

[21] A. S. Chou, W. Wester, A. Baumbaugh, H. R. Gustafson, Y. Irizarry-Valle, P. O. Mazur, J. H. Steffen, R. Tomlin, X. Yang, and J. Yoo, Phys. Rev. Lett. **100** 080402(4) (2008).

[22] A. Afanasev, O. K. Baker, K. B. Beard, G. Biallas, J. Boyce, M. Minarni, R. Ramdon, M. Shinn, and P. Slocum, Phys. Rev. Lett. **101** 120401 (2008)

[23] Pierre Pugnat, Lionel Duvillaret, Remy Jost, Guy Vitrant, Daniele Romanini, Andrzej Siemko, Rafik Ballou, Bernard Barbara, Michael Finger, Miroslav Finger, Jan Hošek, Miroslav Král, Krzysztof A. Meissner, Miroslav Šulc, and Josef Zicha, Phys. Rev. D **78**, 092003 (2008)

[24] Several other photon regeneration experiments either in preparation or proposed are found in A. Ringwald, arXiv:hep-ph/0612127.

[25] J.-Y. Vinet, P. Hello, C.N. Man, A. Brillet, J. Phys. (Paris) I **2** 1287-1303 (1992), P. Hello, J.-Y. Vinet, J. Phys. France **51** 1267 (1990), P. Hello, J.-Y. Vinet, J. Phys. France **51** 2243 (1990)

[26] Ryan Lawrence, *Active Wavefront Correction in Laser Interferometric Gravitational Wave Detectors*, Ph.D. thesis, MIT (2003).

[27] A.E. Siegman, *Lasers*, University Science Books, Sausalito, CA (1984).

[28] R.W.P. Drever, J.L. Hall, F.V. Kowalski, J. Hough, G.M. Ford, A.J. Munley, and H. Ward, Appl. Phys. B **31**, 97 (1983); Eric D. Black, Am. J. Phys. **69**, 79 (2001).

[29] ETX-500 data sheet at http://www.jdsu.com/product-literature/etx500_ds_cc_ae.pdf.